Structure-Based Design of Selective Inhibitors of Dihydrofolate Reductase: Synthesis and Antiparasitic Activity of 2,4-Diaminopteridine Analogues with a Bridged Diarylamine Side Chain

Andre Rosowsky,*[,†] Vivian Cody,[‡] Nikolai Galitsky,[‡] Hongning Fu,[†] Andrew T. Papoulis,[†] and Sherry F. Queener[§]

Dana-Farber Cancer Institute and Department of Biological Chemistry and Molecular Pharmacology, Harvard Medical School, Boston, Massachusetts 02115, Hauptman-Woodward Medical Research Institute, Buffalo, New York 14203, and Department of Pharmacology and Toxicology, Indiana University School of Medicine, Indianapolis, Indiana 46202

Received June 25, 1999

As part of a larger search for potent as well as selective inhibitors of dihydrofolate reductase (DHFR) enzymes from opportunistic pathogens found in patients with AIDS and other immune disorders, *N*-[(2,4-diaminopteridin-6-yl)methyl]dibenz[*b*,*f*]azepine (**4a**) and the corresponding dihydrodibenz[*b*,*f*]azepine, dihydroacridine, phenoxazine, phenothiazine, carbazole, and diphenylamine analogues were synthesized from 2,4-diamino-6-(bromomethyl)pteridine in 50−75% yield by reaction with the sodium salts of the amines in dry tetrahydrofuran at room temperature. The products were tested for the ability to inhibit DHFR from *Pneumocystis carinii* (pcDHFR), *Toxoplasma gondii* (tgDHFR), *Mycobacterium avium* (maDHFR), and rat liver (rlDHFR). The member of the series with the best combination of potency and species selectivity was **4a**, with IC_{50} values against the four enzymes of 0.21, 0.043, 0.012, and 4.4 μM, respectively. The dihydroacridine, phenothiazine, and carbazole analogues were also potent, but nonselective. Of the compounds tested, **4a** was the only one to successfully combine the potency of trimetrexate with the selectivity of trimethoprim. Molecular docking simulations using published 3D structural coordinates for the crystalline ternary complexes of pcDHFR and hDHFR suggested a possible structural interpretation for the binding selectivity of **4a** and the lack of selectivity of the other compounds. According to this model, **4a** is selective because of a unique propensity of the seven-membered ring in the dibenz[*b*,*f*]azepine moiety to adopt a puckered orientation that allows it to fit more comfortably into the active site of the *P. carinii* enzyme than into the active site of the human enzyme. Compound **4a** was also evaluated for the ability to be taken up into, and retard the growth of, *P. carinii* and *T. gondii* in culture. The IC_{50} of **4a** against *P. carinii* trophozoites after 7 days of continuous drug treatment was 1.9 μM as compared with previously observed IC_{50} values of >340 μM for trimethoprim and 0.27 μM for trimetrexate. In an assay involving [^{3}H]uracil incorporation into the nuclear DNA of *T. gondii* tachyzoites as the surrogate endpoint for growth, the IC_{50} of **4a** after 5 h of drug exposure was 0.077 μM. The favorable combination of potency and enzyme selectivity shown by **4a** suggests that this novel structure may be an interesting lead for structure−activity optimization.

Introduction

A high incidence of potentially life-threatening opportunistic infections in patients with AIDS has been a marker of this disease ever since it was first defined as a clinical syndrome in the early 1980s. Indeed, clinical diagnosis of acute AIDS is typically made when an HIV-1 positive patient presents with a *Pneumocystis carinii* or *Toxoplasma gondii* infection.[1] A number of other opportunistic pathogens which are not ordinarily a problem in healthy individuals can wreak havoc when normal immune function has been damaged via systematic eradication of T-cells by the AIDS virus. Thus, in addition to the use of reverse transcriptase and protease inhibitors to keep viral replication in check,[2] adjunctive antimicrobial therapy, including chemoprophylaxis, is recognized to have a key role in extending and improving the quality of life of AIDS patients.

Drugs currently prescribed for the therapy and prophylaxis of *P. carinii* pneumonia fall into several classes, of which a prominent group consists of lipophilic antifolates (reviewed in refs 3a,b). Although other lipophilic dihydrofolate reductase (DHFR) inhibitors such as trimetrexate (**1**)[4] and piritrexim (**2**)[5] (Chart 1) have been tested in controlled clinical settings to treat or prevent pneumocystis pneumonia in AIDS patients, the one used most routinely for the treatment of this disease is the antibacterial agent trimethoprim (TMP, **3**).[6]

Because TMP is not very effective against *P. carinii* and other parasitic organisms, a sulfonamide inhibitor of de novo folate synthesis is generally also included.[6] A problem with the use of sulfa drugs in this context, however, is the occurrence in some patients of cutaneous side effects which may not respond to corticosteroids and can be severe enough to require interruption of therapy.[7]

† Dana-Farber Cancer Institute.
‡ Hauptman-Woodward Medical Research Institute.
§ Indiana University.

10.1021/jm990331q CCC: $18.00
Published on Web 10/22/1999

Chart 1

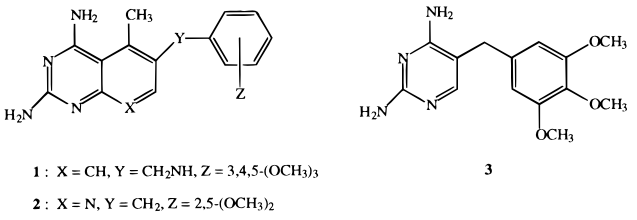

Thus there have been active efforts to develop alternative lipophilic DHFR inhibitors which are potent enough to be used without a sulfa drug and yet are selective enough in their affinity for *P. carinii* versus mammalian DHFR to not require leucovorin co-administration to protect the hematopoietic system of the host.[4,5] Although a large number of lipophilic DHFR inhibitors featuring the monocyclic or condensed diaminopyrimidine motif have been synthesized and a number of them have been quite potent and in some cases fairly selective, an antifolate to challenge the clinical supremacy of the trimethoprim/sulfonamide combination remains to be found.

Synthetic programs directed toward the design of new lipophilic DHFR inhibitors[8−10] have most often followed an empirical medicinal chemistry approach involving, for example, replacement of ring nitrogens by carbon or replacement of a six-membered ring by a five-membered ring. However recent successes in the cloning, expression, and characterization of *P. carinii* DHFR (pcDHFR),[11] and ultimately in the elucidation of the 3D structure of enzyme−inhibitor complexes by X-ray crystallography,[12] have paved the way for more rational structure-based approaches to the design of inhibitors.[13,14] In the present paper we offer an example of the use of structure-based design to generate a novel series of DHFR inhibitors with two rotationally restricted phenyl groups on the bridge nitrogen.

Consideration of the known coordinates for the 3D structures of crystalline pcDHFR and human DHFR (hDHFR)[12] suggests that the hydrophobic cavity defined by the van der Waals surfaces of the active site is somewhat larger in the *P. carinii* enzyme and can therefore accommodate a ligand with a bulkier side chain. Molecular docking simulations with ligands containing a variety of bulky hydrophobic side chains were carried out using the known crystallographic coordinates for the ternary complex of pcDHFR with NADPH and a tight-binding classical inhibitor. An intriguing hypothesis which sprang from these simulations was that compounds with *two* phenyl groups on N^{10}, instead of one as is more typically found in small-molecule antifolates, might fit better into the active site of pcDHFR than into that of hDHFR. Moreover, as discussed in greater detail below, these simulations suggested that locking the two phenyl rings into a rotationally restricted configuration by a bridge might favor selectivity. To test this hypothesis we synthesized a pilot series of 2,4-diaminopteridines of general structure **4** (Scheme 1), in which the X bridge would define the dihedral angle between the phenyl rings. With the phenyl rings joined directly (X = direct link) the tricyclic moiety would be completely planar, whereas a one-atom (X = CH_2, O, S) or two-atom (X = CH_2CH_2, CH=CH) bridge would lead to a chairlike conformation as dictated by the least-strain requirement for six- and seven-membered rings.

Scheme 1

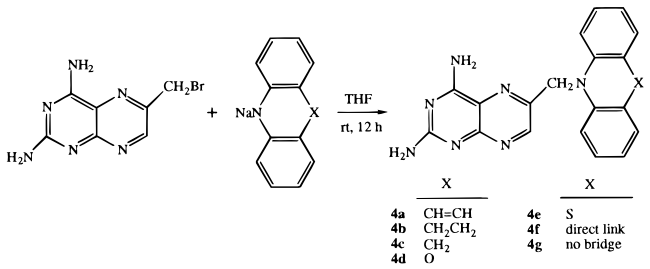

Chemical Synthesis

Facile access to compounds of general structure **4** was made possibly by a straightforward modification of the method of Piper and Montgomery.[15] As shown in Scheme 1, alkylation of the nucleophilic nitrogen anion of dibenz[*b*,*f*]azepine (iminostilbene), 9,10-dihydrodibenz[*b*,*f*]azepine (iminodibenzyl), 9,10-dihydroacridine (acridan), phenothiazine, phenoxazine, or carbazole with 2,4-diamino-6-(bromomethyl)pteridine hydrobromide (**5**·HBr) in dry THF at room temperature afforded the bridged *N*,*N*-diarylamine derivatives **4a**−**f**, respectively. The same reaction using *N*,*N*-diphenylamine led to the nonbridged analogue **4g**. Because of the low nucleophilicity of the diarylamines, it was necessary to first convert them to the corresponding anions with NaH. A good solvent for the reaction was found to be THF, though care had to be taken to dry the solvent and keep the reaction mixture under a blanket of dry N_2 in order to exclude moisture. The molar ratio of the amine to the bromide salt **5**·HBr was 2:1, and the NaH was likewise used in excess (5.4 mol/mol of **5**·HBr). Purification was satisfactorily achieved by flash chromatography and/or preparative TLC on silica gel. The products were yellow powders except in the case of the phenoxazine **4d** and the phenothiazine **4e**, whose colors had an orange-yellow and greenish-yellow tinge, respectively. Purified yields ranged from 39% (**4b**) to 78% (**4a**) and were most often around 50%. ^{1}H NMR spectra of the products, measured in DMSO-d_6 solution, displayed the expected C^9 bridge protons as a singlet at ca. 5.3 ppm and the C^7 pteridine ring proton as a singlet between 8.5 and 8.9 ppm. In the case of **4a**−**c**, **4f**, and **4g**, structural assignments were also corroborated by mass spectrometric analysis, which revealed the expected M + 1 peak as the major species.

Biochemical and Biological Assays

The ability of **4a**−**g** to inhibit partly purified pcDHFR and *T. gondii* DHFR (tgDHFR), as well as their selectivity for these enzymes versus rat liver DHFR (rlDHFR), was determined as previously described.[16] As with many lipophilic DHFR inhibitors, the low aqueous solubility of these compounds necessitated the use of DMSO to prepare concentrated stock solutions. Rat liver enzyme was used because (i) immunosuppressed rats are typically the primary in vivo model for drugs against *P. carinii*;[17] (ii) a full sequence for the rat enzyme has not been reported, but comparative N-terminal analysis of the purified rat[18a] and human[18b] proteins indicates substantial sequence homology (including especially the

Table 1. Inhibition of DHFR by *N*-[(2,4-Diaminopteridin-6-yl)methyl]dibenz[*b*,*f*]azepine (**4a**) and Related Compounds with a Bulky Bridged *N*,*N*-Diarylamine Side Chain

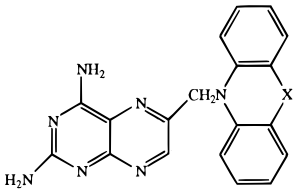

				DHFR inhibition (IC_{50}, μM)[b]				selectivity ratio[c]		
compd	X	potency[a]	selectivity[a]	pc	tg	ma	rl	rl/pc	rl/tg	rl/ma
type 1		low	high							
trimethoprim (**3**)[f]				12	2.7	0.19[e]	130	11	48	680
type 2		low	low							
4b	CH_2CH_2			1.4	0.91		5.1	3.6	5.6	
4d	O			3.4	2.2	2.5	13	3.8	5.9	5.2
4g	none			4.9	1.3	3.7	4.0	0.82	3.1	1.1
type 3		high	low							
trimetrexate (**1**)[d]				0.042	0.01		0.003	0.07	0.30	
4c	CH_2			0.042	0.029	0.017	0.027	0.64	0.93	1.6
4e	S			0.12	0.11	0.029	0.20	1.7	1.8	6.9
4f	direct			0.10	0.012		0.055	0.55	4.6	
type 4		high	high							
4a	CH=CH			0.21[e]	0.043[e]	0.012	4.4[f]	21	102	367

[a] Low potency is arbitrarily defined here as an IC_{50} of >1.0 μM, high potency as an IC_{50} of <0.1 μM; the difference between low and high selectivity is arbitrarily set at a selectivity index of 10. [b] Replicate assays performed as previously described.[16] [c] Defined as the ratio IC_{50}(rat)/IC_{50}(*P. carinii* or *T. gondii*). [d] Data cited, for example, in ref 10b. [e] Mean of two sets of titrations done on different days. [f] Mean of four sets of titrations on different days.

Asp21 residue which distinguishes pcDHFR from mammalian DHFRs); and (iii) inhibitors generally bind similarly to both enzymes.[19] Thus, even though a crystal structure for the rat enzyme is not yet available and our simulations were based on published coordinates for ternary complexes of the human protein,[12] we assume that binding affinities of **4a**−**g** for rlDHFR are a reasonable portrayal of their interaction with hDHFR.

As shown in Table 1, a rather wide range of potency was observed among compounds **4a**−**g** against both pcDHFR and tgDHFR. The most potent members of the series were the dihydroacridine **4c**, the phenothiazine **4e**, and the carbazole **4f**, with IC_{50} values of 0.01−0.1 μM; the least potent were the dihydrodibenz[*b*,*f*]azepine **4b** (CH_2CH_2 bridge), the phenothiazine **4d** (O bridge), and the diphenylamine **4g** (no bridge), with IC_{50} values of >1.0 μM. The IC_{50} of **4e** (S bridge) was lower than that of either **4d** (O bridge) or **4b** (CH_2CH_2 bridge) but higher than that of **4c** (CH_2 bridge). When the effect of a bridge versus no bridge was considered, potency was increased by direct covalent linkage of the two phenyl rings or by insertion of a CH_2, S, or CH=CH bridge, but not by insertion of a CH_2CH_2 or O bridge.

The pattern of activity of **4a**−**g** against rlDHFR paralleled their pattern of activity against pcDHFR, but **4a** showed a 20-fold preference for the latter enzyme even though it was less potent than several other analogues (Table 1). To the extent that it tended to support the hypothesis that differences in bulk tolerance within the active site of DHFR from different species can be exploited in the structure-based design of new antifolates selective for *P. carinii*, this finding was very encouraging. However an even more gratifying outcome of the studies was that **4a**, apart from being moderately selective for pcDHFR, displayed 100-fold selectivity against tgDHFR. Moreover, when **4a** was tested against *Mycobacterium avium* DHFR (maDHFR), the enzyme of another opportunistic pathogen often found in AIDS patients and other immunosuppressed individuals, its IC_{50} was found to be 0.012 μM. Thus the enzyme selectivities of **4a** for maDHFR and tgDHFR appear to be of the same order. Two other members of the series, **4c** and **4e**, likewise showed excellent activity against maDHFR (Table 1), with IC_{50} values of 0.017 and 0.029 μM. However because these compounds were also potent against rlDHFR, they lacked the selectivity of **4a**. It is of interest that the possibility that small-molecule antifolates which are active against *P. carinii* and *T. gondii* may be useful as drugs against *M. avium* complex has recently been suggested in two other reports.[14b,20]

Overall, compounds **4a**−**g** can be seen to fall into four categories which we have arbitrarily defined as type 1 (low potency/high selectivity), type 2 (low potency/low selectivity), type 3 (high potency/low selectivity), and type 4 (high potency/high selectivity). Prototypical examples of the first and third category are trimethoprim (**3**) and trimetrexate (**1**), respectively. The relative potencies and selectivities of **3** and **1** against pcDHFR and rlDHFR were consistent with their previously reported kinetic inhibition constants (K_i values) against pcDHFR and hDHFR.[11d] Interestingly, **4b**−**g** were all either more potent than **3** or more selective than **1**, whereas only **4a** displayed both of these characteristics and therefore could be said to belong to type 4. Thus an important goal of future work with these compounds would be to find more examples of type 4.

Because of its promising combination of potency and selectivity, **4a** was also tested as an inhibitor of the growth of *P. carinii* organisms cultured on confluent layers of human embryonic lung (HEL) fibroblasts in the presence of 10 μM folic acid as previously described.[17a,c] In a pilot experiment in which the cells were continuously exposed to **4a** for 7 days at a concentration of 1.0

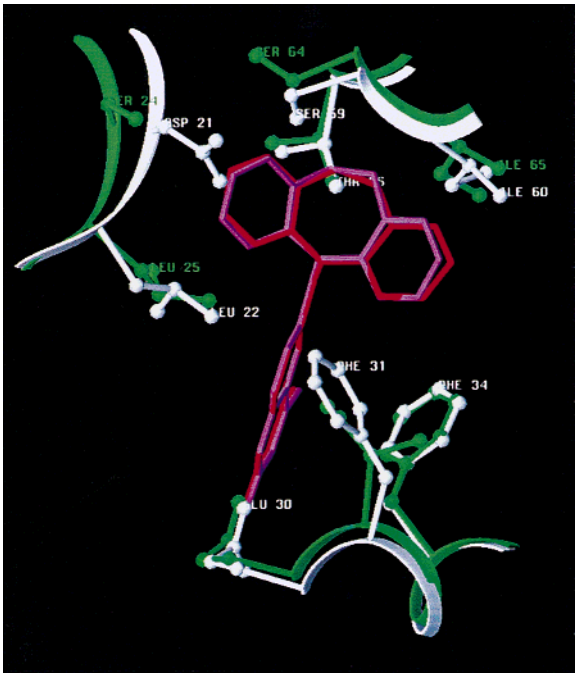

Figure 1. Computer-generated model of the sterically disfavored 'a' orientation of **4a** (pink structure) and **4b** (red structure) in the active site of pcDHFR (green) and hDHFR (white). The illustrations were made with the program SETOR.[24] Note that, in this orientation, while pcDHFR has better contacts, there are many more unfavorable contacts through this region of the active site.

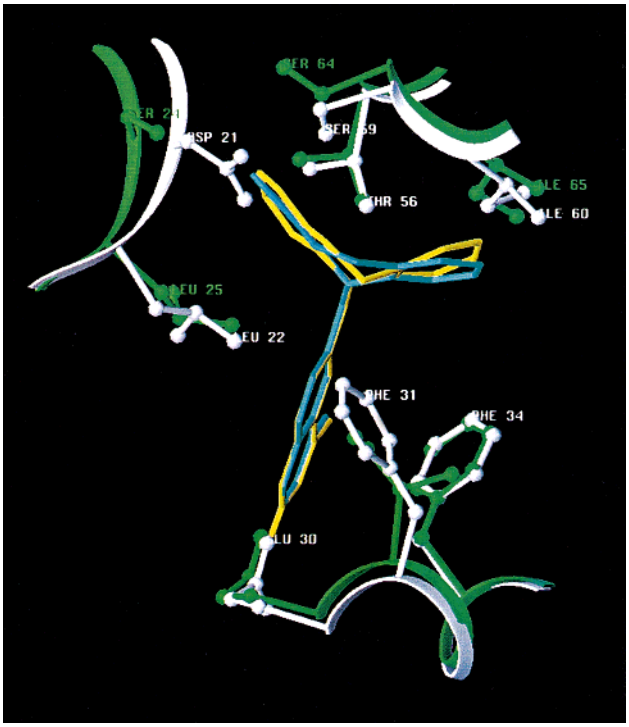

Figure 2. Computer-generated model of the sterically favored 'b' orientation of **4a** (cyan structure) and **4b** (yellow structure) in the active site of pcDHFR (green) and hDHFR (white). The illustrations were made with the program SETOR.[24] Note that, in this orientation, **4a** has better contacts to the pcDHFR active site than to the human enzyme and that the contacts to both enzymes are more favorable than those of the 'a' orientation in Figure 1.

or 10 μM, a >75% decrease in growth relative to untreated controls was observed, whereas at 0.1 μM the drug was inactive. As expected from the inclusion of a high concentration of folic acid in the medium, no evidence of toxicity to the HEL cells was noted. The IC_{50} was estimated to be 1.9 μM. Trimethoprim (**3**) alone has almost no effect on the growth of *P. carinii* in culture even at 340 μM.[17a] In contrast, the reported IC_{50} of trimetrexate (**1**) is 0.27 μM.[3a] Thus the potency of **4a** in this assay was intermediate between that of **1** and that of **3**, but closer to that of **1**. When the effect of the drug was assessed via metabolic incorporation of [^{3}H]*p*-aminobenzoic acid into the total folate pool of *P. carinii* organisms as described by Kovacs and co-workers,[21] treatment with **4a** at a concentration of 18 μM for 5 h resulted in a 62% decrease in radioactivity relative to untreated controls. The fact that much more **4a** was required to inhibit the growth of the intact trophozoites than to inhibit isolated DHFR suggests that uptake into the parasite is not very efficient, as has been noted for other lipophilic DHFR inhibitors.[17c]

Growth inhibition assays were also performed against *T. gondii* tachyzoites in culture as previously described,[17c] using an assay based on incorporation of [^{3}H]uracil into the nuclear DNA of the parasite after a drug exposure time of 24 h. The IC_{50} value of **4a** in this surrogate assay of growth was 0.077 μM. The IC_{50} of **4b** was 0.69 μM, in reasonable agreement with the difference in IC_{50} that had been observed between **4a** and **4b** in the tgDHFR inhibition assay.

On the basis of the foregoing biochemical and biological results, it appears that the dibenzazepine derivative **4a** may be an interesting lead for further development. However it is obvious that neither selective DHFR binding nor the ability to inhibit parasitemia in culture can guarantee that a compound will be efficacious in vivo. Thus, any future assessment of the clinical potential of **4a** or one of its second-generation analogues would have to address its mode of administration, pharmacokinetics, tissue distribution, and other pharmacologic characteristics. While these issues are clearly important, they were not considered to fall within the scope of the present work.

Simulated Interaction of Inhibitors with DHFR

Models of the binding of **4a**−**c**, **4e**, and **4f** to the active site of pcDHFR were generated by using the molecular graphics program Sybyl[22] to 'replace' the tight-binding inhibitor methotrexate (MTX) in the corresponding enzyme complexes of known structure,[12b] as was done recently to simulate the interaction of another series of small-molecule inhibitors with pcDHFR.[23] A significant feature of compounds of general structure **4** is that inversion of the pyramidal ring nitrogen can cause the tricyclic moiety to adopt different spatial orientations relative to the pteridine ring. Because the topology of these limiting orientations is especially important in the dibenzazepine derivatives **4a** and **4b**, a stereoscopic image for one of these orientations (called 'a') is displayed in Figure 1, whereas the other (called 'b') is given in Figure 2. Key amino acids in the active site of the *P. carinii* enzyme are marked in green, and their homologous residues in the human enzyme are marked in white. As required by the docking strategy, the pteridine ring in both orientations of **4a** and **4b** in the ternary complex with NADPH is essentially superimposable on

the diaminopteridine moiety of MTX, allowing the 2-amino group to interact in the usual manner with the γ-carboxyl group of human Glu30 and *P. carinii* Glu32. Prominent differences in the *P. carinii* enzyme contributing to its sterically more permissive active site relative to the human enzyme are the substitution of Ile33 for Phe31 and of Ser24 for Asp21. Of particular note is that the Asp21 side chain in hDHFR points toward the inhibitor, whereas the Ser24 side chain in pcDHFR is rotated out of the way, creating an empty cavity into which the inhibitor can comfortably fit. A difference can also be seen in the permissive arrangement of Ser64 and Ile65 in pcDHFR relative to Ser59 and Ile60 in hDHFR. Of greatest interest, however, is that in the 'a' orientation the tricyclic moiety of **4a** (Figure 1, pink structure) and **4b** (Figure 1, red structure) lies prohibitively close to the serine and isoleucine side chains of each enzyme, whereas in the 'b' orientation (Figure 2; **4a**, cyan structure; **4b**, yellow structure) the edge rather than the face of the tricyclic moiety is turned toward the viewer. It was evident from these models that **4a** and **4b** should bind better to the enzyme in orientation 'b'. This distinctive spatial realignment of the tricyclic moiety via inversion of the pyramidal ring nitrogen, analogous to the flapping of butterfly wings, is only possible when the central ring is seven-membered. Thus, while inversion of this nitrogen does occur in the other tricyclic systems (**4c**−**f**), as well as in the nonbridged analogue **4g**, only in **4a** and **4b** does this inversion bring about the same steric relief.

A comparison of the simulated contact distances between the bound ligand and several key amino acid residues in the active site of hDHFR (Leu22, Asp21, Phe31, Ser59, Ile60) and pcDHFR (Leu25, Ile33, Ser64, Ile65) was carried out for the 'a' and 'b' orientations of **4a** and **4b**, as well as for the other analogues in which nitrogen inversion cannot afford the same degree of topologic change as it does in the seven-membered ring structures. A detailed listing of these simulated distances is given in Table 2 (see Supporting Information). The Ser24 side chain of pcDHFR was excluded from the analysis because, in contrast to the Asp21 of the human enzyme, it faces away from the ligand. Generally speaking, simulated contact distances of <2.5 Å are considered to be sterically disfavored, whereas distances of 2.5−3.0 Å are viewed as borderline, and distances of 3.0−3.5 Å are preferred. Using the 'a' and 'b' orientations of **4a** as an illustration, a number of the predicted contact distances turn out to be <2.5 Å in the 'a' orientation, whereas in the 'b' orientation the number of such distances is zero. For example the nearest predicted contact for the aromatic carbons next to the CH═CH bridge in the 'a' orientation of **4a** is the β-carbon of Ser59 in hDHFR (2.1 Å) and Ser64 in pcDHFR (2.7 Å). The corresponding distances in the 'b' orientation are 3.1 and 3.6 Å, respectively. Thus, for the atoms used in this particular comparison, it can easily be seen that (i) the 'a' orientation is less favorable than the 'b' orientation where both enzymes are concerned, and (ii) even in the 'b' orientation, the *P. carinii* enzyme appears to be favored over the human enzyme. Similar analysis of other predicted distances for **4a** and **4b** (cf. Table 2, Supporting Information) leads to the same general conclusion. In contrast, analysis of predicted contact distances for the other compounds (**4d**−**g**) does not reval this species difference. Thus we were led to speculate that **4a** and **4b** may show greater species selectivity than the other rotationally restricted compounds in the series, for which the same opportunity to gain steric relief via inversion of the pyramidal ring nitrogen does not seem to exist.

Computer simulation was also used to model the interaction of the Asp21 side chain of hDHFR with **4a** and the other members of the series. As indicated in Table 2 (Supporting Information), while the aromatic carbon *ortho* to the CH═CH bridge of **4a** is 3.1 Å from the β-carbon of Ser59, this aromatic carbon also lies near the β-COOH of Asp21, with a predicted contact distance of 2.7 Å in the 'a' orientation and 3.1 Å in the 'b' orientation. Thus, in the sterically preferred 'b' orientation, this carbon is equidistant from the β-COOH of Asp21 and the β-carbon of Ser59. However, because there is no counterpart for the Asp21 interaction in the *P. carinii* enzyme, we feel that this interaction may be less important than the one involving Ser59 in conferring selectivity.

An important qualification has to be made whenever docking simulations of small molecules to enzymes or other complex protein structures are performed, namely that consideration of a protein as a rigid structure may lead to an oversimplified view of the system. Thus, a drawback of such a static model is that it does not take into account the possibility that the DHFR can undergo a ligand-induced conformational change of its 3D structure. To rigorously address this issue, a docking experiment needs to be followed up with a real (as opposed to 'virtual') structural analysis of the enzyme−inhibitor complex. To this end, work is currently in progress to crystallize and solve the structure of the ternary complex of **4a** with pcDHFR. Modeling experiments using second-generation analogues of **4a** would likewise be of potential interest.

Experimental Section

IR spectra were obtained on a Perkin-Elmer model 781 double-beam recording spectrophotometer. Only peaks above 1200 cm^{-1} are reported; weak peaks and shoulders are omitted. ^1H NMR spectra were recorded at 60 MHz on a Varian model EM360 instrument using Me_4Si as the reference or on a 500 MHz Varian VX 500 instrument. When they were seen, NH_2 peaks were broad signals at δ 6.6 and 7.6 and could be eliminated by adding a drop of D_2O. Mass spectra in the electron-impact (EI) or fast-atom bombardment (FAB) mode were provided by the Molecular Biology Core Facility of the Dana-Farber Cancer Institute. Reported M + 1 peaks were major species in each case. Analytical TLC was on Whatman MK6F silica gel plates, and preparative separations were on Aldrich TLC plates (fluorescent silica gel, 1000-μm layer, 20 × 20 cm). TLC spots were visualized under a UV lamp at 254 nm. Column chromatography was on Baker 7024 flash silica gel (40-μm particle size). 2,4-Diamino-6-(bromomethyl)pteridine hydrobromide (**5**·HBr) was obtained as the *i*-PrOH solvate as reported in the literature[15] and for simplicity is referred to as **5**·HBr. The amount of *i*-PrOH in each batch was estimated by microanalysis or examination of the ^1H NMR spectrum, and the amount of material used in each reaction was adjusted to correct for variations in the estimated amount of *i*-PrOH in the sample. 9,10-Dihydroacridine (acridan) was obtained from acridine in 70% yield by hydrogenation in the presence of Raney Ni and was recrystallized from MeOH in the form of colorless needles: mp 169−170 °C (lit.[25] mp 170 °C). Other chemicals were purchased from Aldrich or Fisher; all the diarylamines were dried in vacuo at 60 °C overnight before

use. The THF for the *N*-alkylation reactions was distilled from Na and dibenzophenone and was stored over Linde 4A molecular sieves. Melting points were determined in Pyrex capillary tubes using a Mel-Temp apparatus (Laboratory Devices, Inc., Cambridge, MA) and are not corrected. Samples for microanalysis were dried in a vacuum oven at 70 °C overnight. Elemental analyses were performed by QTI Laboratories, Whitehouse, NJ, or Robertson Microlit Laboratories, Madison, NJ, and were within ±0.4% of theoretical values unless otherwise noted.

***N*-[(2,4-Diaminopteridin-6-yl)methyl]dibenz[*b,f*]azepine (4a).** A stirred solution of dibenz[*b,f*]azepine (78 mg, 0.404 mmol) in dry THF (10 mL) was purged at 0 °C with a gentle stream of dry N_2 (5 min) and treated with a single portion of powdered NaH (95%, 51 mg, 2.13 mmol). After another 10 min of stirring, **5**·HBr (100 mg, 0.392 mmol) was added and the flask was fitted with a balloon of N_2, allowed to come to room temperature, and left to stir for another 12 h, during which the color changed from greenish-yellow to brilliant yellow. After decomposition of the excess NaH by dropwise addition of MeOH (2 mL), the mixture was concentrated to dryness by rotary evaporation at 45 °C (bath temperature). Flash chromatography on silica gel (95:5 $CHCl_3$−MeOH) gave **4a** as a yellow powder which was dried in vacuo at 70 °C overnight: yield 113 mg (78%); mp 251 °C dec; MS (FAB) *m*/*z* (M + 1) = 368; IR (KBr) ν 3430, 3290, 3180, 3100, 1620, 1600, 1575, 1550, 1470, 1440, 1350 cm^{-1}; ^1H NMR (DMSO-d_6) δ 5.20 (s, 2H, 9-CH_2), 6.80−7.40 (complex m, 1H, CH=CH and aryl ring protons), 8.75 (s, 1H, C_7−H). Anal. ($C_{21}H_{17}N_7$·0.5CH_3OH) C, H, N.

The following compounds were obtained by essentially the same method as described for the synthesis of **4a**.

***N*-[(2,4-Diaminopteridin-6-yl)methyl]-9,10-dihydrodibenz[*b,f*]azepine (4b).** Excess NaH in the reaction was quenched by dropwise addition of a mixture of MeOH (1 mL) and glacial AcOH (0.2 mL). After the solvents were removed by rotary evaporation at 45 °C (bath temperature), the residue was purified by preparative TLC (4:1 $CHCl_3$−MeOH) to obtain **4b** as a yellow powder in 39% yield: mp 275 °C dec; MS (FAB) *m*/*z* (M + 1) = 370; IR (KBr) ν 3450, 3300, 3220, 1610, 1555, 1480, 1440, 1360, 1220 cm^{-1}; ^1H NMR (DMSO-d_6) δ 3.35 (s, 4H, CH_2CH_2), 5.15 (s, 2H, bridge CH_2), 6.80−7.40 (m, 8H, aromatic protons), 8.80 (s, 1H, C_7−H). Anal. ($C_{21}H_{19}N_7$·0.5CH_3-OH) C, H, N.

***N*-[(2,4-Diaminopteridin-6-yl)methyl]-9,10-dihydroacridine (4c).** The crude product after evaporation of the THF was taken up in 9:1 $CHCl_3$−MeOH (40 mL), preadsorbed onto silica gel (2 g), and applied to the top of a flash chromatography column, which was eluted with 95:5 followed by 9:1 $CHCl_3$−MeOH. Appropriately pooled fractions were repurified on a standard gravity column (95:5 $CHCl_3$−MeOH) to obtain **4c** as a yellow solid in 50% yield: mp 222−224 °C dec; IR (KBr) ν 3450, 3370, 3320, 3200, 1640, 1615, 1590, 1560, 1480, 1440, 1360 cm^{-1}; ^1H NMR (DMSO-d_6) δ 4.21 (s, 2H, ring CH_2), 5.30 (s, 2H, bridge CH_2), 6.50−7.50 (m, 8H, aromatic protons), 8.37 (s, 1H, C_7−H); MS (FAB) *m*/*z* (M + 1) = 370. Anal. ($C_{20}H_{17}N_7$·0.5H_2O) C, H, N.

***N*-[(2,4-Diaminopteridin-6-yl)methyl]phenoxazine (4d).** The crude product after evaporation of the THF was purified by flash chromatography (9:1 $CHCl_3$−MeOH) followed by preparative TLC (4:1 $CHCl_3$−MeOH) to obtain **4d** as a brownish yellow solid in 54% yield: mp 250 °C dec; IR (KBr) ν 3440, 3320, 3200, 3060, 1620, 1590, 1560, 1490, 1450, 1370, 1270 cm^{-1}; ^1H NMR (DMSO-d_6) δ 5.02 (s, 2H, bridge CH_2), 6.60−6.90 (m, 8H, aromatic protons), 8.70 (s, 1H, C_7−H). Anal. ($C_{19}H_{15}N_7O$·0.5CH_3OH) C, H, N.

***N*-[(2,4-Diaminopteridin-6-yl)methyl]phenothiazine (4e).** The crude product after evaporation of the THF was purified by flash chromatography on silica gel (9:1 $CHCl_3$−MeOH) followed by preparative TLC (4:1 $CHCl_3$−MeOH) to obtain **4e** as a greenish-yellow powder in 44% yield: mp 232−234 °C dec; IR (KBr) ν 3450, 3380, 3310, 3200, 1630, 1590, 1560, 1540, 1450, 1360, 1220 cm^{-1}; ^1H NMR (DMSO-d_6) δ 5.30 (s, 2H, bridge CH_2), 6.80−7.40 (m, 8H, aromatic protons), 8.60 (s, 1H, C_7−H). Anal. ($C_{19}H_{15}N_7S$·0.7CH_3OH) C, H, N.

***N*-[(2,4-Diaminopteridin-6-yl)methyl]carbazole (4f).** The crude product after evaporation of the THF was purified flash chromatography (95:5 $CHCl_3$−MeOH) to obtain **4f** as a bright-yellow powder in 59% yield: mp 267 °C dec; IR (KBr) ν 3440, 3340, 3200, 1610, 1555, 1480, 1445, 1450, 1320, 1205 cm^{-1}; ^1H NMR (DMSO-d_6) δ 5.75 (s, 2H, bridge CH_2), 7.10−8.25 (m, 8H, aromatic protons), 8.45 (s, 1H, C_7−H); (MS FAB) *m*/*z* (M + 1) = 342. Anal. ($C_{19}H_{15}N_7$·0.5H_2O) C, H, N.

***N*-[(2,4-Diaminopteridin-6-yl)methyl]-*N*,*N*-diphenylamine (4g).** The crude product after evaporation of the THF was purified by flash chromatography (95:5 $CHCl_3$−MeOH) to obtain **4g** as a bright-yellow powder in 43% yield: mp >250 °C dec; MS (FAB) *m*/*z* (M + 1) = 344; IR (KBr) ν 3450, 3340, 3170, 1630, 1590, 1550, 1490, 1450, 1360, 1220 cm^{-1}; ^1H NMR (DMSO-d_6) δ 5.10 (s, 2H, CH_2), 6.70 (m, 10H, aromatic protons), 8.60 (s, 1H, C_7−H). Anal. ($C_{19}H_{17}N_7$·0.8H_2O) C, H, N.

DHFR Assays. The previously described spectrophotometric assay was used to measure the ability of compounds **4a**−**g** to decrease the rate of enzymic reduction of dihydrofolate to tetrahydrofolate in the presence of NADPH.[16] The standard assay mixture contained 0.092 mM dihydrofolate, 0.117 mM NADPH, 8.9 mM 2-mercaptoethanol, and 3.7 IU of enzyme (1 IU = 0.005 optical density units/min) in 40.7 mM sodium phosphate buffer, pH 7.4, in a total volume of 1.0 mL. The assay mixture in the experiments using maDHFR also contained 150 mM KCl. The enzyme was obtained from a clinical isolate of *M. avium* ('serovar 4') as described earlier[26] and contained both DHFR and dihydropteroate synthase activity.

As an illustration of the reproducibility of the DHFR assays, the IC_{50} values (mean ± standard error) obtained over a recent 5-year period in Dr. Queener's laboratory with pyrimethamine against pcDHFR, tgDHFR, and rlDHFR have been 2.50 ± 0.23, 1.52 ± 0.32, and 2.39 ± 0.42 μM, respectively.

Modeling Studies of DHFR Binding. Molecular docking simulations for compounds **4a**−**g** into the active site of pcDHFR and hDHFR were performed with the help of the builder function of the Sybyl program[22] using the standard minimizer function and were similar to others we recently reported.[23] Models were made with the SETOR program.[24] Recently analyzed crystal structures of the complexes of MTX with pcDHFR and hDHFR[12c] were used in fitting the analogues into the active site. The preliminary fit was made by superimposing the diaminopteridine ring of the analogue onto the diaminopteridine ring of MTX.

Acknowledgment. This work was supported in part by Grants RO1-AI29904 (A.R.) and RO1-GM51670 (V.C.) and by Contract NO1-AI35171 (S.F.Q.) from the National Institutes of Health, DHHS.

Supporting Information Available: Predicted contact distances for the side-chain tricyclic moiety of compounds **4a**−**g** with several key residues in pcDHFR and hDHFR. This material is available free of charge via the Internet at http://pubs.acs.org.

References

(1) (a) Falloon, J.; Masur, H. Infectious complications of HIV. In *AIDS Etiology, Diagnosis, Treatment and Prevention*, 3rd ed.; DeVita, V. T., Hellman, S., Rosenberg, S. A., Eds.; Lippincott: Philadelphia, 1992. (b) Klepser, M. E.; Klepser, T. B. Drug treatment of HIV-related opportunistic infections. *Drugs* **1997**, *53*, 40−73.

(2) DeClercq, E. Toward improved anti-HIV chemotherapy: therapeutic strategies for intervention with HIV infections. *J. Med. Chem.* **1995**, *38*, 2491−1517.

(3) (a) Queener, S. F. New drug developments for opportunistic infections in immunocompromised patients: *Pneumocystis carinii*. *J. Med. Chem.* **1995**, *38*, 4739−4759. (b) Gangjee, A.; Elzein, E.; Kothare, M.; Vasudevan, A. Classical and nonclassical antifolates as potential antipneumocystis and antitoxoplasma agents. *Curr. Pharm. Des.* **1996**, *2*, 263−280.

(4) (a) Allegra, C. J.; Chabner, B. A.; Tuazon, C. U.; Ogata-Arakaki, D.; Baird, B.; Drake, J. C.; Simmons, J. T.; Lack, E. E.; Shelhamer, J. H.; Balis, F.; Walker, R.; Kovacs, J. A.; Lane, H. C.; Masur. H. Trimetrexate for the treatment of *Pneumocystis carinii* pneumonia in patients with the acquired immunodeficiency syndrome. *N. Engl. J. Med.* **1987**, *317*, 978−985. (b) Sattler, F. R.; Frame, P.; Davis, R.; Nichols, L.; Shelton, B.; Akil, B.; Baughman, R.; Hughlett, C.; Weiss, W.; Boylen, C. T.; van der Horst, C.; Black, J.; Powderly, W.; Steigbigel, R. T.; Leedom, J. M.; Masur, H.; Feinberg, J.; Benoit, S.; Eyste, E.; Gocke, D.; Beck, K.; Lederman, M.; Phari, J.; Reichman, R.; Sacks, H. S.; Soiero, R. Trimetrexate with leucovorin versus trimethoprim-sulfamethoxazole for moderate to severe episodes of *Pneumocystis carinii* pneumonia in patients with AIDS - - a prospective controlled multicenter investigation of the AIDS clinical trials group Protocol 029/031. *J. Infect. Dis.* **1994**, *170*, 165−172.

(5) Falloon, J.; Allegra, C. J.; Kovacs, J.; O'Neill, D.; Ogata-Arakaki, D.; Feuerstein, I.; Polis, M.; Davey, R.; Lane, H. C.; LaFon, S.; Rogers, M.; Zunich, K.; Turlo, J.; Tuazon, C.; Parenti, D.; Simon, G.; Masur, H. Piritrexim with leucovorin for the treatment of pneumocystis pneumonia (PCP) in AIDS patients. *Clin. Res.* **1990**, *38*, 361A.

(6) (a) Fischl, M. A.; Dickinson, G. M.; La Voie, L. Safety and efficacy of sulfamethoxazole and trimethoprim chemoprophylaxis for *Pneumocystis carinii* pneumonia in AIDS. *J. Am. Med. Assoc.* **1988**, *105*, 45−48. (b) Medina, I.; Mills, J.; Leoung, G.; Hopewell, P. C.; Modin, G.; Benowitz, N.; Wofsy, C. B. Oral therapy for *Pneumocystis carinii* pneumonia in the acquired immunodeficiency syndrome. A controlled trial of trimethoprim-sulfamethoxazole versus trimethoprim-dapsone. *N. Engl. J. Med.* **1990**, *323*, 776−782. (c) Podzamczer, D.; Salazar, A.; Jimenes, J.; Santin, M.; Consiglio, E.; Casanova, A.; Rufi, G.; Gudiol, F. Intermittent trimethoprim-sulfamethoxazole compared with dapsone-pyrimethamine for the simultaneous prophylaxis of Pneumocystis pneumonia and toxoplasmosis in patients infected with HIV. *Ann. Intern. Med.* **1995**, *122*, 755−761.

(7) (a) Caumes, E.; Roudier, C.; Rogeaux, O.; Bricaire, F.; Gentilini, M. Effect of corticosteroids on the incidence of adverse cutaneous reactions to trimethoprim-sulfamethoxazole associated *Pneumocystis carinii* pneumonia. *Clin. Infect. Dis.* **1994**, *17*, 319−323. (b) Roudier, C.; Caumes, E.; Rogeauz, O.; Bricaire, F.; Gentilini, M. Adverse cutaneous reactions to trimethoprim-sulfamethoxazole in patients with the acquired immunodeficiency syndrome and *Pneumocystis carinii* pneumonia. *Arch. Dermatol.* **1994**, *30*, 1383−1386.

(8) (a) Gangjee, A.; Devraj, R.; Queener, S. F. Synthesis and dihydrofolate reductase activities of 2,4-diamino-5-deaza and 2,4-diamino-5,10-dideaza lipophilic antifolates. *J. Med. Chem.* **1997**, *40*, 470−478. [For earlier papers from this group in this area, see ref 3a; for recent papers from other groups, see refs 9 and 10.] (b) Gangjee, A.; Vasudevan, A.; Queener, S. F. Synthesis and biological evaluation of nonclassical 2,4-diamino-5-methylpyrido[2,3-*d*]pyrimidines with novel side chain substituents as potential inhibitors of dihydrofolate reductases. *J. Med. Chem.* **1997**, *40*, 479−485. (c) Gangjee, A.; Madvandadi, F.; Queener, S. F. Effect of N^9-methylation and bridge atom variation on the activity of 5-substituted 2,4-diaminopyrrolo[2,3-*d*]pyrimidines against dihydrofolate reductases from *Pneumocystis carinii* and *Toxoplasma gondii*. *J. Med. Chem.* **1997**, *40*, 1173−1177. (d) Gangjee, A.; Shi, J.; Queener, S. F. Synthesis and biological activities of conformationally restricted, tricyclic nonclassical antifolates as inhibitors of dihydrofolate reductases. *J. Med. Chem.* **1997**, *40*, 1930−1936. (e) Gangjee, A.; Vasudevan, A.; Queener, S. F. Conformationally restricted analogues of trimethoprim: 2,6-diamino-8-substituted purines as potential dihydrofolate reductase inhibitors from *Pneumocystis carinii* and *Toxoplasma gondii*. *J. Med. Chem.* **1997**, *40*, 3032−3039.

(9) (a) Piper, J. R.; Johnson, C. A.; Krauth, C. A.; Carter, R. L.; Hosmer, C. A.; Queener, S. F.; Borotz, S. E.; Pfefferkorn, E. R. Lipophilic antifolates as agents against opportunistic infections. 1. Agents superior to trimetrexate and piritrexim against *Toxoplasma gondii* and *Pneumocystis carinii* in in vitro evaluations. *J. Med. Chem.* **1996**, *39*, 1271−1280. (b) Jackson, H. C.; Biggadike, K.; McKillingin, E.; Kinsman, O. S.; Queener, S. F.; Lane, A.; Smith, J. E. 6,7-Disubstituted 2,4-diaminopteridines: novel inhibitors of *Pneumocystis carinii* and *Toxoplasma gondii* dihydrofolate reductase. *Antimcirob. Agents Chemother.* **1996**, *40*, 1371−1374. (c) Robson, C.; Meek, M. A.; Grundwaldt, J.-D.; Lambert, P. A.; Queener, S. F.; Schmidt, D.; Griffin, R. J. Nonclassical 2,4-diamino-5-aryl-6-ethylpyrimidine antifolates: activity as inhibitors of dihydrofolate reductase from *Pneumocystis carinii* and *Toxoplasma gondii* and as antitumor agents. *J. Med. Chem.* **1997**, *40*, 3040−3048.

(10) (a) Rosowsky, A.; Mota, C. E.; Queener, S. F. Brominated trimetrexate analogues as inhibitors of *Pneumocystis carinii* and *Toxoplasma gondii* dihydrofolate reductase. *J. Heterocycl. Chem.* **1996**, *33*, 1959−1966. [For earlier papers from this group in this area, see ref 3a.] (b) Rosowsky, A.; Papoulis, A. T.; Queener, S. F. 2,4-Diaminothieno[2,3-*d*]pyrimidine lipophilic antifolates as inhibitors of *Pneumocystis carinii* and *Toxoplasma gondii* dihydrofolate reductase. *J. Med. Chem.* **1997**, *40*, 3694−3699. (c) Rosowsky, A.; Forsch, R. A.; Queener, S. F. Synthesis of 2,4-diaminopteridines with bulky lipophilic groups at the 6-position as inhibitors of *Pneumocystis carinii*, *Toxoplasma gondii*, and mammalian dihydrofolate reductase. *Pteridines* **1997**, *8*, 173−187. (d) Rosowsky, A.; Papoulis, A. T.; Queener, S. F. 2,4-Diamino-6,7-dihydro-5*H*-cyclopenta[*d*]pyrimidine analogues of trimethoprim as inhibitors of *Pneumocystis carinii* and *Toxoplasma gondii* dihydrofolate reductase. *J. Med. Chem.* **1998**, *41*, 913−918. (e) Rosowsky, A.; Papoulis, A. T.; Forsch, R. A.; Queener, S. F. Synthesis and antiparasitic and antitumor activity of 2,4-diamino-6-(arylmethyl)-5,6,7,8-tetrahydroquinazoline analogues of piritrexim. *J. Med. Chem.* **1999**, *42*, 1007−1017. (f) Rosowsky, A.; Papoulis, A. T.; Queener, S. F. One-step synthesis of novel 2,4-diaminopyrimidine antifolates from bridged alicyclic ketones and cyanoguanidine. *J. Heterocycl. Chem.* **1999**, *36*, 723−728.

(11) (a) Edman, J. C.; Edman, U.; Cao, M.; Lundgren, B.; Kovacs, J. A.; Santi, D. V. Isolation and expression of the *Pneumocystis carinii* dihydrofolate reductase gene. *Proc. Natl. Acad. Sci. U.S.A.* **1989**, *86*, 8625−8629. (b) Sirawaraporn, W.; Edman, J. C.; Santi, D. V. Purification and properties of recombinant *Pneumocystis carinii* dihydrofolate reductase. *Protein Express. Purif.* **1991**, *2*, 313−316. (c) Delves, C. J.; Ballantine, C. P.; Tansik, R. L.; Baccanari, D. P. Stammers, D. K. Refolding of recombinant *Pneumocystis carinii* dihydrofolate reductase and characterization of the enzyme. *Protein Express. Purif.* **1993**, *4*, 16−23. (d) Margosiak, S. A.; Appleman, J. R.; Santi, D. V. Blakley, R. L. Dihydrofolate reductase from the pathogenic fungus *Pneumocystis carinii*: catalytic properties and interaction with antifolates. *Arch. Biochem. Biophys.* **1993**, *305*, 499−508.

(12) (a) Champness, J. N.; Achari, A.; Ballantine, S. P.; Bryant, P. K.; Delves, C. J.; Stammers, D. K. The structure of *Pneumocystis carinii* dihydrofolate reductase to 1.9 Å resolution. *Structure* **1994**, *2*, 915−924. (b) Cody, V.; Galitsky, N.; Luft, J. R.; Pangborn, W.; Gangjee, A.; Devraj, R.; Queener, S. F.; Blakley, R. L. Comparison of ternary complexes of *Pneumocystis carinii* and wild-type human dihydrofolate reductase with a novel classical antitumor furo[2,3-*d*]pyrimidine antifolate. *Acta Crystallogr. D* **1997**, *D53*, 638−649. (c) Cody, V.; Galitsky, N.; Rak, D.; Luft, J. R.; Pangborn, W.; Queener, S. F. Ligand-induced conformational changes in the crystal structures of *Pneumocystis carinii* dihydrofolate reductase complexes with folate and $NADP^+$. *Biochemistry* **1999**, *38*, 4304−4312.

(13) (a) Southerland, W. M. A molecular model of the folate binding site of *Pneumocystis carinii* dihydrofolate reductase. *J. Comput.-Aided Mol. Des.* **1994**, *8*, 113−122. (b) Geschwend, D. A.; Good, A. C.; Kuntz, I. D. Molecular docking towards drug discovery. *J. Mol. Recognit.* **1996**, *9*, 175−186. (c) Geschwend, D. A.; Sirawaraporn, W.; Santi, D. V.; Kuntz, I. D. Specificity in structure-based design: identification of a novel, selective inhibitor of *Pneumocystis carinii* dihydrofolate reductase. *Proteins* **1997**, *29*, 59−67.

(14) (a) Gangjee, A.; Guo, X.; Queener, S. F.; Cody, V.; Galitsky, N.; Luft, J. R.; Pangborn, W. Selective *Pneumocystis carinii* dihydrofolate reductase inhibitors: design, synthesis, and biological evaluation of new 2,4-diamino-5-substituted-furo[2,3-*d*]pyrimidines. *J. Med. Chem.* **1998**, *44*, 1263−1271. (b) Gangjee, A.; Elzein, E.; Queener, S. F.; McGuire, J. J. Synthesis and biological activities of tricyclic conformationally restricted tetrahydropyrido annulated furo[2,3-*d*]pyrimidines as inhibitors of dihydrofolate reductases. *J. Med. Chem.* **1998**, *41*, 1409−1416. (c) Gangjee, A.; Vidwans, A. P.; Vasudevan, A.; Queener, S. F.; Kisliuk, R. L.; Cody, V.; Li, R.; Galitsky, N.; Luft, J. R.; Pangborn, W. Structure-based design and synthesis of lipophilic 2,4-diamino-6-substituted quinazolines and their evaluation as inhibitors of dihydrofolate reductases and potential antitumor agents. *J. Med. Chem.* **1998**, *41*, 3426−3434.

(15) Piper, J. R.; Montgomery, J. A. Preparation of 6-(bromomethyl)-2,4-pteridinediamine hydrobromide and its use in improved syntheses of methotrexate and related compounds. *J. Org. Chem.* **1977**, *42*, 208−210.

(16) (a) Broughton, M. C.; Queener, S. F. *Pneumocystis carinii* dihydrofolate reductase used to screen potential antipneumocystis drugs. *Antimicrob. Agents Chemother.* **1991**, *35*, 1348−1355. (b) Chio, L.-C.; Queener, S. F. Identification of highly potent and selective inhibitors of *Toxoplasma gondii* dihydrofolate reductase. *Antimicrob. Agents Chemother.* **1993**, *37*, 1914−1923.

(17) (a) Queener, S. F.; Bartlett, M. S.; Jay, M. A.; Durkin, M. M.; Smith, J. W. Activity of lipid-soluble inhibitors of dihydrofolate reductase against *Pneumocystis carinii* in culture and in a rat model of infection. *Antimicrob. Agents Chemother.* **1987**, *31*, 1323−1327. (b) Kovacs, J. A.; Allegra, C. J.; Kennedy, S.; Swan, J. C.; Drake, J.; Parrillo, J. E.; Chabner, B.; Masur, H. Efficacy of trimetrexate, a potent lipid-soluble antifolate, in the treatment of rodent *Pneumocystis carinii* pneumonia. *Am. J. Trop. Med.*

Hyg. **1988**, *39*, 491−496. (c) Bartlett, M. S.; Shaw, M.; Navaran, P.; Smith, J. W.; Queener, S. F. Evaluation of potent inhibitors of dihydrofolate reductase in a culture model for growth of *Pneumocystis carinii*. *Antimicrob. Agents Chemother*. **1995**, *39*, 2436−2441.

(18) (a) Johnson, S. J.; Gupta, S. V.; Stevenson, K. J.; Freisheim, J. H. Purification and characterization of dihydrofolate reductase from Walker 256 carcinosarcoma. *Can. J. Biochem*. **1982**, *60*, 1132−1142. (b) Delcamp, T. J.; Susten, S. S.; Blankenship, D. T.; Freisheim, J. H. Purification and characterization of dihydrofolate reductase from methotrexate-resistant human lymphoblastoid cells. *Biochemistry* **1983**, *22*, 633−639.

(19) Burchall, J. J.; Hitchings, G. H. Inhibitor binding analysis of dihydrofolate reductases from various species. *Mol. Pharmacol*. **1965**, *1*, 126−136.

(20) Shoen, C. M.; Choromanska, O.; Reynolds, R. C.; Piper, J. R.; Johnson, C. A.; Cynamon, M. H. In vitro activities of several diaminomethylpyridopyrimidines *against Mycobacterium avium* complex. *Antimicrob. Agents Chemother*. **1998**, *42*, 3315−3316.

(21) Kovacs, J. A.; Allegra, C. J.; Beaver, J.; Boarman, D.; Lewis, M.; Parrillo, J. E.; Chabner, B.; Masur, H. Characterization of de novo folate synthesis in *Pneumocystis carinii* and *Toxoplasma gondii*: potential for screening therapeutic agents. *J. Infect. Dis*. **1989**, *160*, 312−320.

(22) Tripos, Inc., 1699 S. Handley Rd., Suite 303, St. Louis, MO 63144.

(23) Rosowsky, A.; Queener, S. F.; Cody V. Inhibition of dihydrofolate reductases from *Toxoplasma gondii*, *Pneumocystis carinii*, and rat liver by rotationally restricted analogues of pyrimethamine and metoprine. *Drug Des. Discovery* **1999**, *16*, 25−40.

(24) Evans, S. V. SETOR. *J. Mol. Graph*. **1993**, *11*, 148−153.

(25) Tarnoky, A. L. Some properties of acridane and 2-chloro-7-methoxyacridane: their possible relationships to excretion product of mepacrine. *Biochem. J*. **1950**, *46*, 297−300.

(26) Chio, L.-C.; Boylard, L. A.; Nasr, M.; Queener, S. F. Identification of a class of sulfonamides highly active against dihydropteroate synthase from *Toxoplasma gondii*, *Pneumocystis carinii*, and *Mycobacterium avium*. *Antimicrob. Agents Chemother*. **1996**, *40*, 727−733.

JM990331Q